Study on the effectiveness of integrated methodologies for determining thermophysical properties of building envelope structures

Renat Sadykov, Airat Osipov, Artem Akhmerov , Aida Mukhametzianova
[1] Kazan State Power Engineering University, st. Krasnoselskaya, 51, 420066, Kazan, Russia
E-mail: sadykov_r_a@mail.ru, nord7077@yandex.ru, akhm@mail.ru

Abstract: *To design energy-efficient buildings, it is essential to accurately calculate, monitor, and analyze their energy consumption at all stages: from conceptual (sketch) development and design to construction and operation. However, current regulatory documentation lacks methodologies that fully account for the interrelated processes occurring in building envelopes—such as heat transfer, moisture accumulation, and air infiltration—evaluate the effectiveness of specific energy-saving measures, or perform energy consumption data analysis to determine a building's actual energy performance indicators.This highlights the relevance of calculating and analyzing building energy consumption while accounting for heat and mass transfer processes in envelope structures and the presence of various architectural and construction elements. A methodology has been developed for processing data obtained from building thermal energy metering systems. This methodology allows, during the operational phase, to determine buildings' energy characteristics, evaluate the efficiency of thermal energy use, and assess the effectiveness of energy-saving measures.*

KEY WORDS: *SHORT-TERM CONTACT, MATHEMATICAL MODELING, SYSTEMS OF DIFFERENTIAL EQUATIONS, POTENTIALS, PHASES, MODES, VECTOR, MATRIX, HEAT AND MASS TRANSFER, COEFFICIENTS.*

1. Introduction

One type of energy-efficient building is the Passive House (Passivhaus). Passive Houses are buildings with extremely low energy demand, where annual heating energy consumption does not exceed 15 kWh/(m²·year), and heat losses through the building envelope are limited to a U-value ≤ 0.15 W/(m²·K).

Achieving these targets is impossible without using high-performance thermal insulation with a thermal conductivity $\lambda <$ 0.030 W/(m·K), as well as design solutions that minimize thermal bridges and ensure airtightness.

Over the past five years, rapid advancements have been observed both in innovative insulation materials and intelligent insulation systems that combine energy efficiency, environmental sustainability, and durability.

2. Review of New Thermal Insulation Materials

Vacuum Insulation Panels (VIPs) remain at the forefront of thermal protection materials due to their exceptionally low thermal conductivity—ranging from 0.004 to 0.008 W/(m·K)—which is 5–10 times lower than that of conventional insulators [1].

Although VIPs were initially limited by high costs and significant degradation risks if the vacuum envelope was damaged, substantial progress in the 2020s has significantly improved their reliability, greatly expanding their application scope [2].

Researchers at Fraunhofer IBP have developed innovative VIPs with multilayer barrier envelopes based on recyclable polymers and nanofibrillated cellulose cores, extending the projected service life to over 30 years, even under high humidity and mechanical stress [1]. These panels are especially effective in thermal bridge-prone areas—such as window reveals and balcony junctions—and in historic building retrofits where wall thickness is critically constrained.

Silica aerogels, with thermal conductivity $\lambda \approx$ 0.012–0.018 W/(m·K) and famously known as "solid smoke" due to their ultra-low density, have evolved from fragile monolithic forms to flexible composite blankets compatible with timber frames, curved surfaces, and render systems [3, 4].

Within the European AEROCOAT project, aerogel-based renders were developed for thermally upgrading historic façades, enabling compliance with Passivhaus standards without altering the building's external appearance, which is essential for structures in protected heritage zones [3].

Environmental sustainability—a core principle of the Passive House concept—has spurred the development of new bio-based materials that significantly outperform traditional cellulose and wood-fiber insulations.

Mycelium composites, made from fungal mycelium and agricultural waste, exhibit thermal conductivity $\lambda \approx$ 0.038–0.045 W/(m·K), are fully biodegradable, and—when properly modified—show good fire resistance [5].

Alginate foams derived from seaweed, developed in 2023, achieved $\lambda \approx$ 0.032 W/(m·K) combined with high moisture resistance—a rare combination for bio-based materials [6].

Compressed straw without synthetic binders is successfully used in monolithic walls, achieving U-values as low as 0.12 W/(m²·K). These materials not only reduce the carbon footprint but also help regulate indoor humidity and improve indoor climate [7].

Metal-Organic Frameworks (MOFs), particularly ZIF-8 (Zeolitic Imidazolate Framework), show strong potential for ultra-low-conductivity insulation. In 2024, researchers at ETH Zürich produced an MOF-based aerogel with λ = 0.011 W/(m·K) and high stability at relative humidity up to 80% [8]. While this technology has not yet reached industrial scale, it paves the way for next-generation "smart" insulation with adaptive properties.

Modern energy-passive houses increasingly employ dynamic insulation systems, notably Dynamic Insulation, in which outdoor air slowly passes through a porous insulation layer, reducing heat losses while providing natural ventilation [9].

Phase Change Materials (PCMs) are integrated into walls and ceilings to smooth daily temperature fluctuations—becoming especially relevant under climate change and increasing cooling demands [10].

3. Current Trends in Determining Envelope Structure Characteristics

According to ISO 9869-1:2014, still widely used today, key experimental methods for determining thermophysical properties include: Heat Flow Meter (HFM) method, Infrared Thermography (IRT), Calibrated Hot Box, Dynamic methods (reducing measurement time from weeks to hours) [11]

Recent years show a clear trend toward hybrid approaches combining multiple methods to improve measurement accuracy—especially under real-world building operating conditions.

Researchers at the Fraunhofer Institute for Building Physics conducted a large-scale field study in 12 certified Passive Houses in Germany, using the HFM method over 14–21 days with a temperature difference of at least 10 K. Results were compared with calculations per DIN EN ISO 6946 and BIM models accounting for thermal bridges [11].

The average deviation between measured and calculated U-values was +8%, indicating systematic underestimation of heat losses in design calculations. The largest discrepancies—up to 25%—occurred at window and balcony slab junctions due to insufficient modeling of linear thermal bridges. However, 3D thermal modeling (using ANSYS or Therm) reduced errors to <5%.

A team from Politecnico di Torino developed an automated thermogram analysis method using convolutional neural networks to estimate U-values and detect anomalies. Tested on 30 buildings (including EnerPHit retrofits), the method achieved ±0.03 W/(m²·K) accuracy versus HFM and successfully identified hidden insulation defects—such as settling and moisture accumulation—that are invisible to visual inspection. Conventional models ignoring defects overestimated insulation performance by 12–18% [12].

Researchers at Empa proposed an accelerated "step heating" method: briefly heating the interior wall surface and analyzing the cooling curve. This reduces measurement time to 6–8 hours instead of the traditional 2–3 weeks. The method was tested on walls with aerogel and wood-fiber insulation, showing <7% deviation from ISO 6946 and HFM for homogeneous constructions. However, for multilayer systems with PCMs, deviations reached 15% due to unaccounted thermal inertia in steady-state calculations [13].

The IEA EBC Annex 80 project (completed in 2024) analyzed 3–5 years of monitoring data from 18 buildings and found that moisture accumulation in bio-based insulation increases thermal conductivity by 10–22%—a factor ignored in standard dry-state material calculations [14]. The authors recommend making dynamic hygrothermal modeling (e.g., using WUFI Pro) a mandatory part of Passive House design in temperate and humid climates.

In summary, modern thermophysical studies confirm that calculated U-values per ISO 6946 are often overly optimistic, especially when thermal bridges, installation defects, or material moisture are present. Thus, on-site measurements are essential to validate design solutions in Passive Houses. 3D thermal bridge modeling per ISO 10211 should become standard practice, not an exception. Dynamic methods and AI-driven technologies significantly accelerate and reduce the cost of diagnostics, enabling mass-scale application. Long-term monitoring—including in-wall humidity and temperature—is necessary to assess a building's true energy performance.

4. Experimental Determination of Thermal Characteristics in a Climatic Chamber

A comprehensive experimental study was conducted on the thermal characteristics of prototype envelope structures and moisture distribution through their thickness.

A climatic chamber (Fig. 1) was used, retrofitted with an internal partition and equipment to maintain set microclimatic parameters in cold and warm compartments.

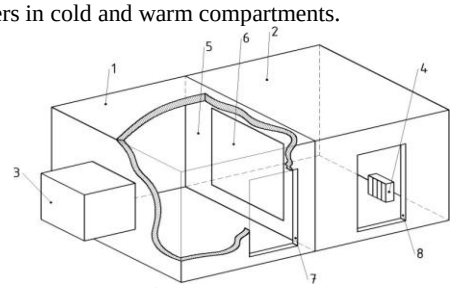

Fig. 1. Layout of the climatic chamber: 1 – cold compartment; 2 – warm compartment;3 – refrigeration unit; 4 – heating device; 5 – dividing wall; 6 – test structure or material; 7, 8 – sealed doors to the cold and warm compartments.

Two types of prototype envelope structures were tested. The goal was to determine the thermo-hygric state of multilayer constructions under varying outdoor temperatures (simulating "cold waves"). Results are shown in Fig. 2, depicting temperature and humidity profiles through the wall thickness at different cold-chamber temperatures.

Thus, under laboratory conditions, "cold waves" of varying intensity and duration—typical of real winter conditions—were successfully replicated.

5. Specimens and Experimental Theirs Thermal Characteristics

Table 1 lists specimen characteristics and table 2 shows boundary conditions. Temperature and relative humidity profiles through the wall at different cold-chamber temperatures are shown in Figs. 2 and 3.Test durations: at t_{ext} = –32°C: 58 h (2.4 days), t_{ext} = –11°C: 100 h (4.2 days), t_{ext} = –20°C: 176 h (7.3 days).

Table 1. Material Characteristics of the Envelope Structure

№	Material	Thickness m	Density kg/m³	Thermal Conductivity W/(m·°C)	Water Vapor Permeability mg/m·h·Pa
1	Plaster	0.015	1800	0.93	0.09
2	Silicate brick masonry	0.25	1800	0.87	0.11
3	ROCKWOOL mineral wool	0.10	90	0.041	0.30

Table 2. Boundary Conditions at Inner and Outer Surfaces

Cold Chamber Temperature, °C	Inner surface		Outter surface	
	t_i, °C	φ_i, %	t_o, °C	φ_o, %
–32	18.1	78	–28.1	88
–11	15.5	54	–8.1	69
–20	14.3	63	–15.5	58

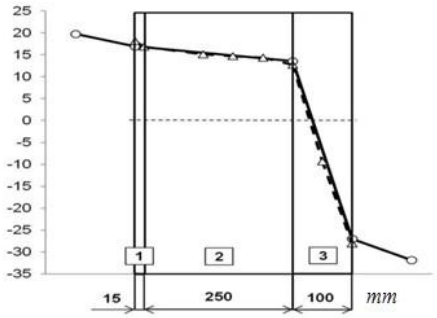

Fig. 2. Temperature distribution through the wall (t_o = –32°C):
1 – plaster, 2 – brick masonry, 3 – mineral wool

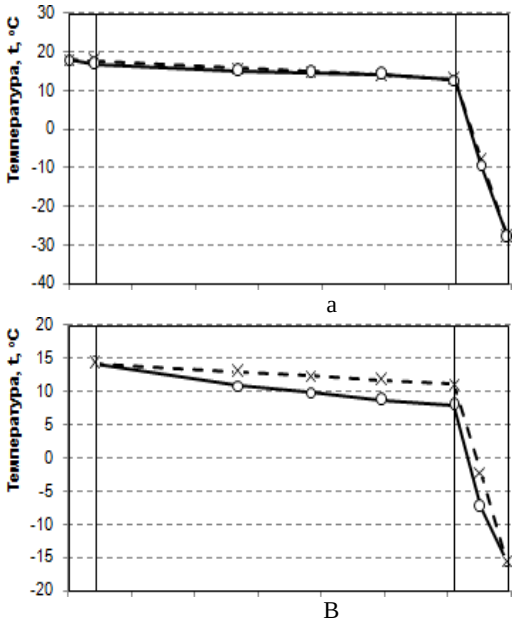

Based on experiments, the following thermal characteristics were determined (Table 3a,b): thermal resistance of brick masonry (R_{bm}) and mineral wool (R_{mv}),thermal conductivity of brick (λ_{bm}) and mineral wool (λ_{mv}), inner surface heat absorption coefficient (α_i) and outer surface heat transfer coefficient (α_o):

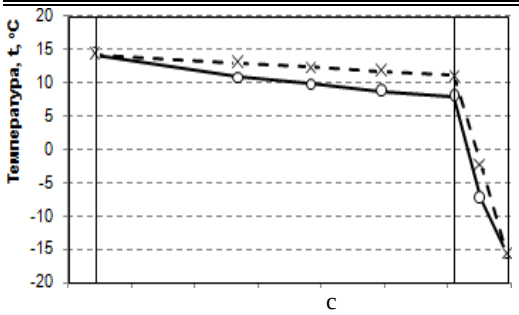

Fig. 3. Temperature profiles under different cold-chamber conditions (solid line – experiment, dashed – calculation):
(a) t_o = –32°C, (b) t_o = –20°C, (c) t_o = –11°C

Table 2. Experimental Thermal Characteristics

Temp, °C	q, W/m²	R_{bm}, m²·°C/W	R_{mv}, m²·°C/W	
–32	32.5	0.128	1.254	
–11	47.8	0.111	0.384	
–20	63.3	0.101	0.370	
Temp, °C	λ_{bm}, W/(m·°C)	λ_{mv}, W/(m·°C)	α_i, W/(m²·°C)	α_o, W/(m²·°C)
–32	1.96	0.08	11.6	6.7
–11	2.25	0.26	5.8	15.9
–20	2.48	0.27	5.3	15.4

6. Mathematical Model of Unsteady Heat Transfer for a Brick Wall Envelope

Problem statement for a brick wall:
Initially, for a brick wall, we have:

$$\begin{cases} t_\tau = at_{xx}, x \in (0,h), \tau \in (0,T) & (1) \\ t(x,0) = f(x) & (2) \\ -\lambda \nabla t(0,\tau) = \alpha_0[\tilde{t}_0 - t(0,\tau)] & (3) \\ -\lambda \nabla t(h,\tau) = \alpha_h[t(h,\tau) - \tilde{t}_h] & (4) \end{cases}$$

In the building envelope, $\nabla_z t = \nabla_y t = 0$; $\nabla_x t \neq 0$ - thermal insulation condition (adiabaticity) of the wall, where $z = H$ - is the height of the building's ES, $y = L$ is the length of the building's ES, $x = h$ – is the thickness of the building's ES, $h \ll L$, $h \ll H$.

Constant but different temperatures are maintained on opposite surfaces of the ES:

$t(0,\tau) = t_{w_1}$;
$t(\delta,\tau) = t_{w_2}$;
and the initial wall temperature $t(x,0) = t_{w_0}$;
$\infty \leftarrow \tau_1 > \tau_2 > \tau_3 > 0$;
$Bi_k \to \infty, k = 1,2;$

$$\begin{cases} t_\tau = at_{xx}, \tau > 0, x \in (0,h) \\ t\,(x,0) = t_0 \\ t\,(0,\tau) = \tilde{t}_0, \;\; t\,(h,\tau) = \tilde{t}_h \end{cases},$$

where α_0, α_h- are the heat transfer coefficients on the opposite surfaces of ES;
$\tilde{t}_0, \tilde{t}_h$ - are the specified temperatures of the external environments;
τ- time, [s];
a – is the thermal diffusivity, [m2 /s];
λ – is the thermal conductivity, [W/m deg];
∇- is the gradient, [1/m];.

The solution of the non-uniform, non-stationary, and asymmetric boundary value problem (1)-(4) under boundary conditions of the first kind ($\alpha_0 \to \infty$,$\alpha_h \to \infty$) by the Fourier method leads to the result:

$$w(x,\tau) = \frac{2}{\pi}(t_0 - \tilde{t}_0)\sum_{n=1}^{\infty}\frac{sin\frac{n\pi x}{h}}{n}e^{\frac{-n^2\pi^2 a\tau}{h^2}} + \frac{2}{\pi}(\tilde{t}_h - t_0)\sum_{n=1}^{\infty}(-1)^n\frac{sin\frac{\pi n x}{h}}{n}\exp\left(-\frac{n^2\pi^2 a\tau}{h^2}\right),$$

$$t(x,\tau) = \tilde{t}_0 - (\tilde{t}_0 - \tilde{t}_h)\frac{x}{h} + w(x,\tau).$$

If only one term n=1 of the series is taken into account:

$$w(x,\tau) \approx w_1 = \frac{2}{\pi}[(t_0 - \tilde{t}_0) - (\tilde{t}_0 - \tilde{t}_h)]e^{\frac{-\pi^2 a\tau}{h^2}}sin\pi\frac{x}{h}$$

Or in dimensionless form

$$\Theta(\eta, Fo) = 1 - \eta + W_1(\eta, Fo)$$

where $\eta = \frac{x}{h}$, $Fo = \frac{a\tau}{h^2}$, $\Theta = \frac{t_0(x,\tau) - \tilde{t}_h}{\tilde{t}_0 - \tilde{t}_h}$,

$$W_1(\eta, Fo) = \frac{1}{\tilde{t}_0 - \tilde{t}_h}w_1(\eta, Fo)$$

Let's assume the following conditions for the problem:
We assume the wall thickness h = 1 meter to simplify the calculations.Thermal diffusivity of brick a = 0.7 m2/s, summation over (n): Approximate calculation of the Fourier series up to 100 terms to achieve sufficient accuracy.

Let's write down the conditions for mathematical modeling of the physical process:
Initial moment $(x,0) = t_0$, the temperature is constant throughout the wall.
Over time $\tau > 0$, the temperature begins to spread from the boundary surfaces to the center of the wall, creating a temperature gradient.
Over a long period of time $\tau \to \infty$, the temperature throughout the wall stabilizes, forming a linear gradient from the inner surface to the outer surface. The initial conditions no longer affect the ES, and the non-stationary process tends toward a quasi-steady-state regime.

Consider the following case, similar to the experimental ones described above, when:

The initial wall temperature $t\,(x,0) = t_0$ is 0 °C.The temperature on the inner surface: $t\,(x,\tau) = \tilde{t}_0,\ \tau = 0$ is +18.1 °C. Temperature on the outer surface $t\,(h,\tau) = \tilde{t}_h, \tau = 0$ is -28.1 °C. In this case, the temperature distribution profile is shown in Figure 4.

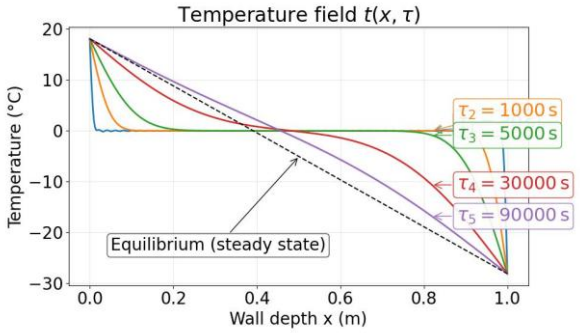

Fig. 4. Temperature profile of a brick wall at unsteady heat transfer:
(a) t_o = +18.1°C, t_h = –28.1°C, (c) t_{wallo}= 0°C

7. Analysis of Experimental Results and Their Numerical Modeling

The temperature field of enclosing temperatures in steady-state mode on the thermal resistance scale is shown in Figure 5. Regression lines (thin solid lines) were plotted for each experimental curve, showing a high degree of agreement with the experimental data (the square of the correlation coefficient is close

to 1), and equations were found in the form of second-degree polynomials. The maximum discrepancy between the calculated and experimental temperatures was: 1.8°C at a temperature in the cold compartment of the spacecraft at -32°C, 4.7°C at -11°C, and 5.2°C at -20°C.

Calculations were also performed using the program algorithm with the data presented in Table 2 (Figure 6).

For this calculation, numerical modeling of non-stationary thermal conductivity was used, specifically the explicit finite difference method, which sequentially updates the temperature at each spatial node based on heat flows from adjacent sections. The discontinuous properties of materials are also taken into account: since the wall consists of two different layers (brick and insulation), their thermal conductivity and heat capacity are defined as piecewise constants. At the boundaries between nodes, thermal conductivity is calculated as the harmonic mean to accurately transfer the heat flux across the material interface. To control the stability of the numerical scheme, the time step is chosen to be small enough to ensure the stability of the calculations, taking into account the maximum thermal diffusivity among the layers. An integral representation of thermal resistance is used instead of a physical coordinate across the wall thickness. The accumulated thermal resistance $Ro = \sum Ri$ from the inner surface is used to plot graphs, allowing for a clear display of the temperature field distribution, accounting for differences in the thermophysical properties of the brick. The steady-state temperature profile t(x) at $\tau = 0$ is calculated separately, for which the heat flux is constant throughout the wall thickness, and is often used for comparison with non-stationary results. The solution domain is divided into a uniform grid across the wall thickness, and the heating/cooling process is modeled step-by-step in time at a given coordinate step (the thickness of the ES). These approaches allow for modeling and visualizing the heating or cooling dynamics of a multilayer ES from the initial state to a steady-state thermal regime.

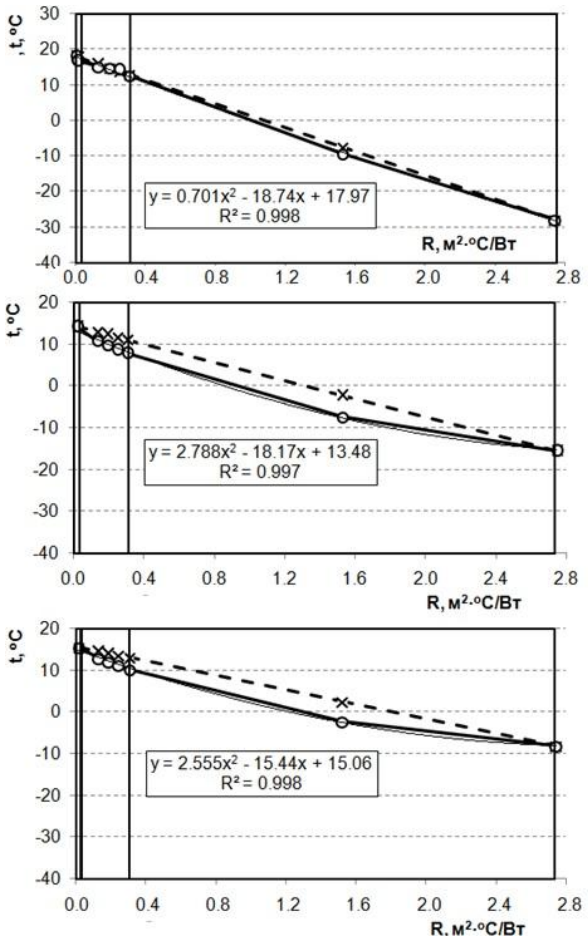

Fig. 5. Temperature profiles under different cold-chamber conditions (solid line – experiment, dashed – calculation):

(a) t_o = –32°C, (b) t_o = –20°C, (c) t_o = –11°C

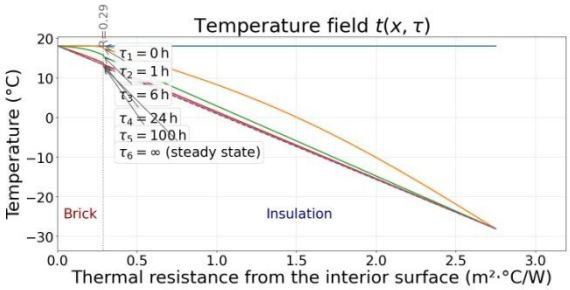

Fig. 6. Temperature profile of a brick wall with insulation at unsteady heat transfer:
(a) t_o = +18.1°C, t_h = –28.1°C, (c) t_{wallo}= +18.1°C

8. Conclusions

These studies confirm that calculation methods for determining the thermal performance of building enclose structure, based on standards, often overestimate the energy efficiency of buildings. This is due to the underestimation of real-world operational factors: thermal bridges, installation defects, moisture accumulation in the insulation, and the dynamic nature of heat and mass transfer. Experimental data obtained in a climate chamber demonstrate significant discrepancies between theoretical and actual values of thermal resistance and thermal conductivity—in some cases, up to 25%.

The developed measurement data processing method, which combines thermography and dynamic approaches with numerical modeling of transient heat transfer, significantly improves the accuracy of assessing the actual thermal performance of structures. The use of hybrid methods for automated diagnostics and detection of hidden defects is particularly promising.

Thus, the transition to truly energy-efficient and sustainable construction requires the unified development of advanced materials, digital diagnostic methods, and dynamic models, using BIM technologies, quantum computers, and technologies that take into account the interrelationships between thermal and moisture exchange processes in enclosing structures at all stages of the life cycle of a building or structure or other multilayer structures, including techno-neural and electrical networks in the fields of power engineering, aerospace engineering, and other industries.

References

1. Caps, R., et al. (2023). Long-term performance and durability of vacuum insulation panels in building envelopes: Field monitoring and accelerated aging. Energy and Buildings, 285, 112918.
2. Baetens, R., Jelle, B. P., & Gustavsen, A. (2010). Vacuum insulation panels for building applications: A review and beyond. Energy and Buildings, 42(2), 147–172.
3. Koebel, M., et al. (2022). Flexible silica aerogel composites for high-performance thermal insulation in retrofit applications. Journal of Non-Crystalline Solids, 595, 121863.
4. Jelle, B. P. (2011). Traditional, state-of-the-art and future thermal building insulation materials and solutions. Energy and Buildings, 43(10), 2549–2563.
5. Jones, M., et al. (2021). Engineered mycelium composite construction materials – A review. Building and Environment, 193, 107653.
6. Briga-Souli, M., et al. (2023). Algae-based biofoams as sustainable thermal insulation materials: Development and characterization. Construction and Building Materials, 398, 132561.
7. Pomianowski, M. Z., et al. (2013). A review of thermal performance of bio-based insulation materials. Energy and Buildings, 65, 34–42.

8. Zhang, Y., et al. (2024). Metal–organic framework aerogels for ultra-low thermal conductivity insulation. Advanced Materials, 36(5), 2307891.
9. Taylor, J., et al. (2020). Dynamic insulation in low-energy buildings: Performance under real-world conditions. Energy and Buildings, 225, 110312.
10. Cabeza, L. F., et al. (2011). Thermal energy storage: Materials, systems and applications. Renewable and Sustainable Energy Reviews, 15(3), 1592–1605.
11. Burch, J., et al. (2023). In-situ U-value measurements in Passive House buildings: Validation of design assumptions and impact of thermal bridges. Energy and Buildings, 294, 113352.
12. Baldinelli, G., et al. (2022). Deep learning-enhanced infrared thermography for in-situ thermal performance assessment of building envelopes. Applied Energy, 328, 120173.
13. Simmler, H., & Brunner, S. (2021). Dynamic in-situ measurement of U-values: Validation of the step heating method on advanced insulation systems. Building and Environment, 205, 108245.
14. Woloszyn, M., et al. (2024). Long-term hygrothermal performance of bio-based insulation in low-energy buildings: Implications for U-value prediction. Energy and Buildings, 301, 113856.